Supplemental Figure 1

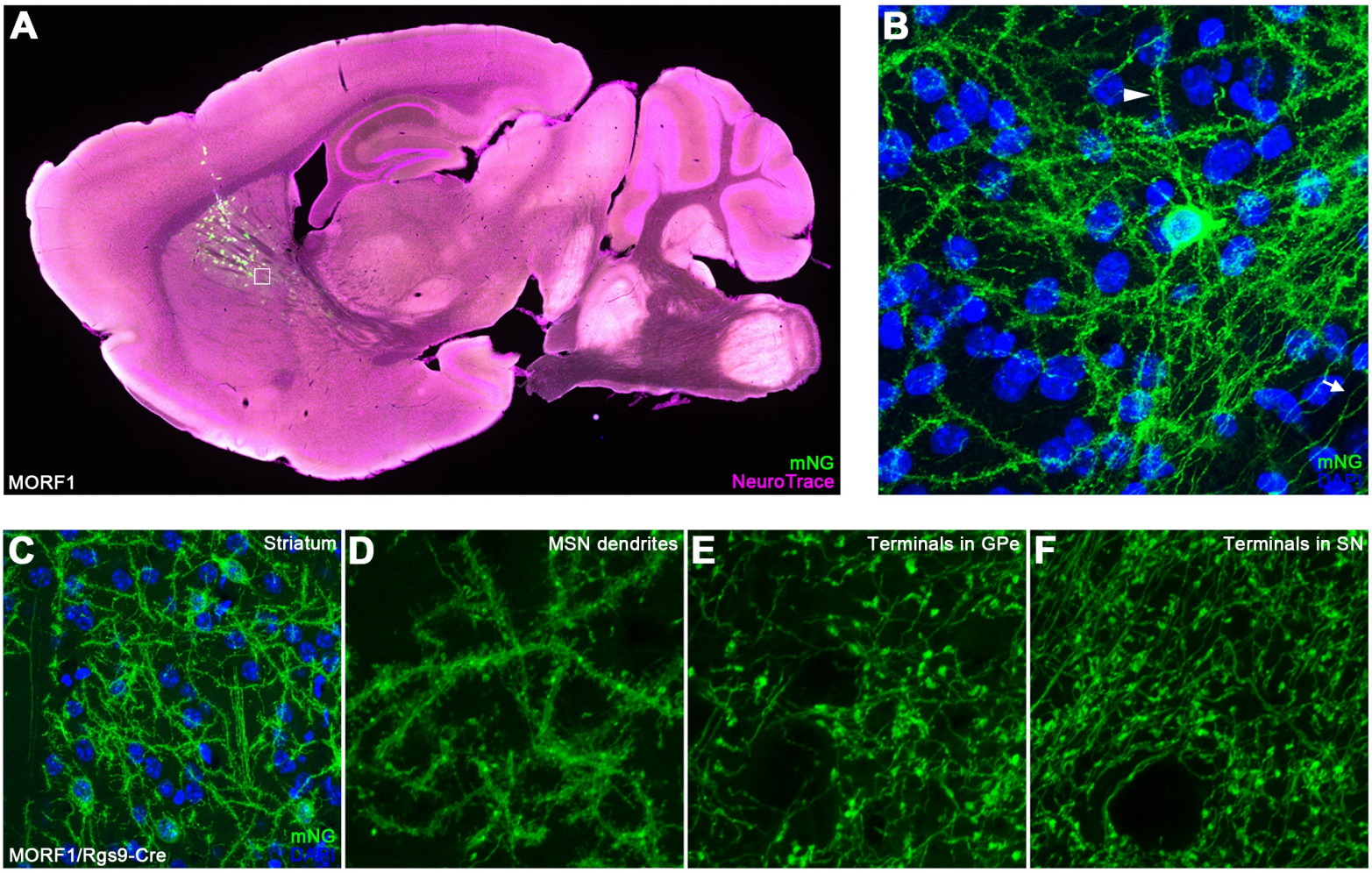

Figure S1. Cre-mediated induction of the MORF1 transgene with AAV-Cre or Rgs9-Cre results in bright and sparse labeling within the basal ganglia. Related to Figure 2. (A) AAV-CMV-Cre-injected striatum of a MORF1 transgenic mouse shows sparse, bright cell labeling with mNeonGreen (endogenous fluorescence) and NeuroTrace counterstain (magenta) in a sagittal section. (B) Within the boxed region in panel A, a higher resolution image of a MSN demonstrating visualization of dendritic spines (arrowhead) and axons (arrow). (C-F) MORF1/Rgs9-Cre labeling of both direct and indirect pathway MSNs in the striatum (C), results in brightly labeled dendritic spines (D), axon terminals in the globus pallidus externus (E) and substantia nigra (F).

Supplemental Figure 2

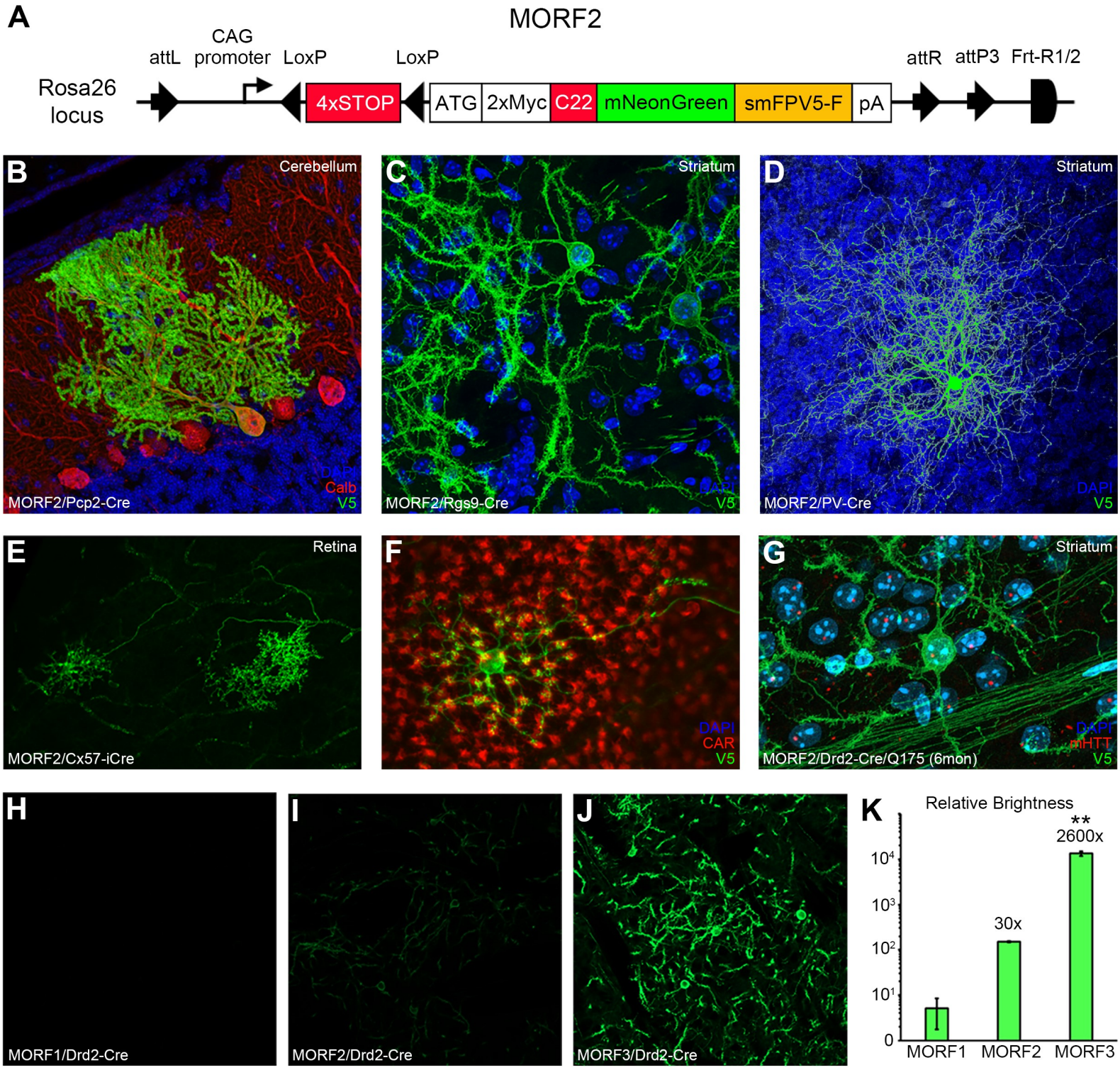

Figure S2. MORF2 transgenic reporter lines brightly and stochastically label immunostained neurons with the smFPV5. Related to Figure 3. (A) Cre-dependent MORF2 transgene design includes an mNeonGreen-smFPV5-fusion protein for membrane localization and immunogenic detection with anti-V5 antibody. (B–D) Immunostaining for V5 of various cell types in double transgenic mice, including cerebellar Purkinje cells in MORF2/Pcp2-Cre (B), striatal MSNs in MORF2/Rgs9-Cre, and parvalbumin interneurons in MORF2/PV-Cre (D). (E and F) Retinal horizontal cells (HC) can be visualized in their entirety in MORF2/Cx57-iCre mice (E), including their dendritic connections to cone cells by double labeling with cone arrestin (CAR; F). (G) Co-labeling of the MORF2 reporter and mutant huntingtin protein (mHTT) aggregates in 6-month-old Q175/MORF2/Drd2-Cre mice demonstrates visualization of cell morphology in a neurodegenerative disease model and stable expression in aging mice. (H-J) MORF3 is magnitudes brighter than MORF1 and MORF2. Images captured at identical exposure setting. (K) Quantification of relative brightness between MORF1 (endogenous fluorescence), MORF2 (immunostained), and MORF3 (immunostained). ** $p<0.01$, ANOVA with Tukey's test, MORF3 versus MORF1 and MORF3 versus MORF2.

Supplemental Figure 3

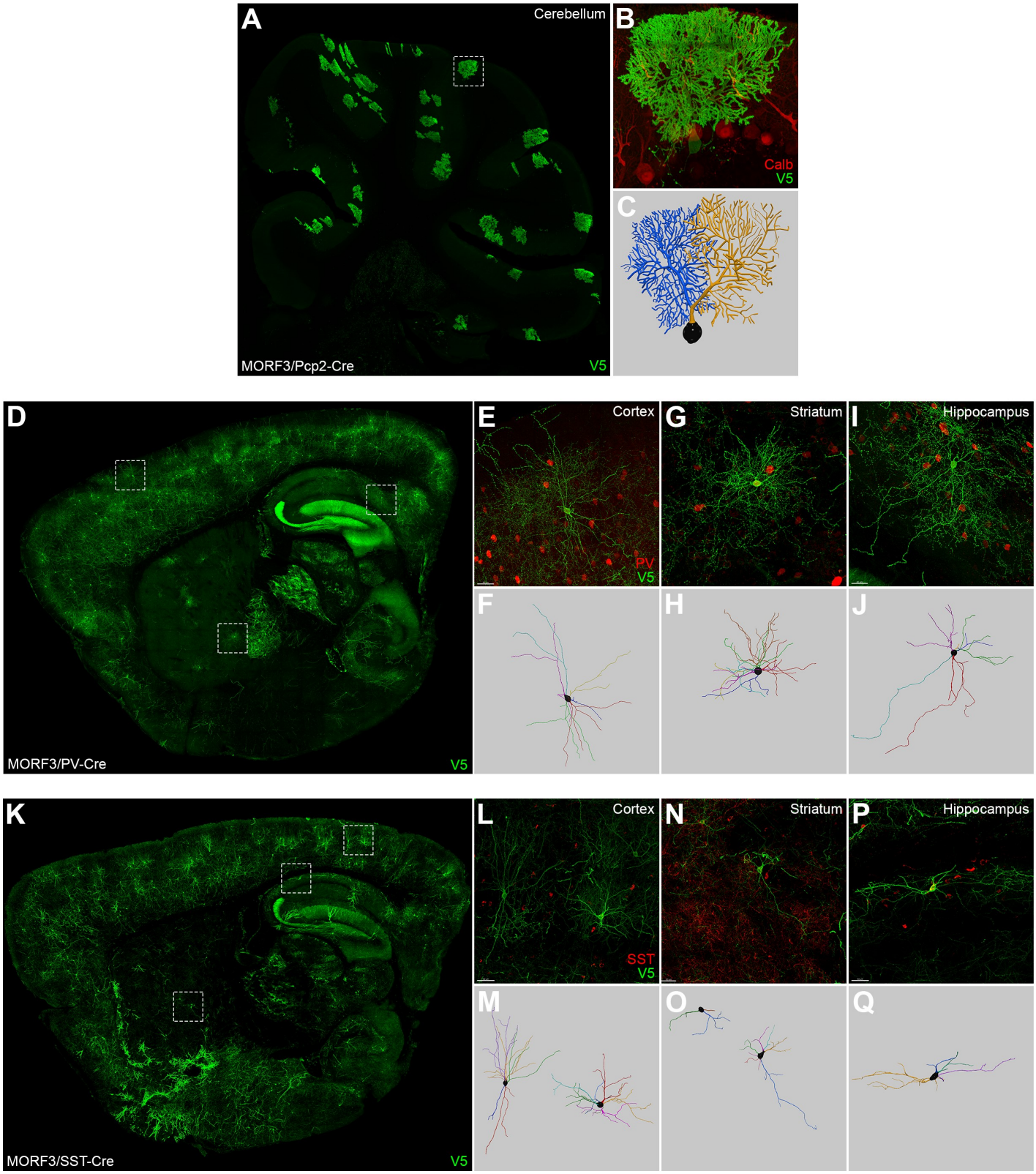

Figure S3. Digital reconstructions of the dendritic morphologies of MORF3 labeled cerebellar Purkinje cells, parvalbumin (PV)- and somatostatin (SST)-expressing interneurons. Related to Figure 3. (A-C) Immunostaining of MORF3-labeled cerebellar Purkinje cells in MORF3/Pcp2-Cre mice (A) allows for detailed imaging of the morphology, including dendrites and axons (B; boxed region in A, co-labeled with calbindin), and digital reconstruction of individual neurons (C). (D) Distribution of PV-expressing interneurons sparsely labeled in MORF3/PV-Cre. (E-J). High magnification (boxed regions in D) of individual MORF3-labeled PV-interneurons, co-labeled with PV, and the corresponding digital reconstructions in the cortex (E and F), striatum (G and H), and hippocampus (I and J). (K) Distribution of SST-expressing interneurons sparsely labeled in MORF3/SST-Cre. (L-Q). High magnification (boxed regions in K) of individual MORF3-labeled SST-interneurons, co-labeled with SST, and the corresponding digital reconstructions in the cortex (L and M), striatum (N and O), and hippocampus (P and Q).

Supplemental Figure 4

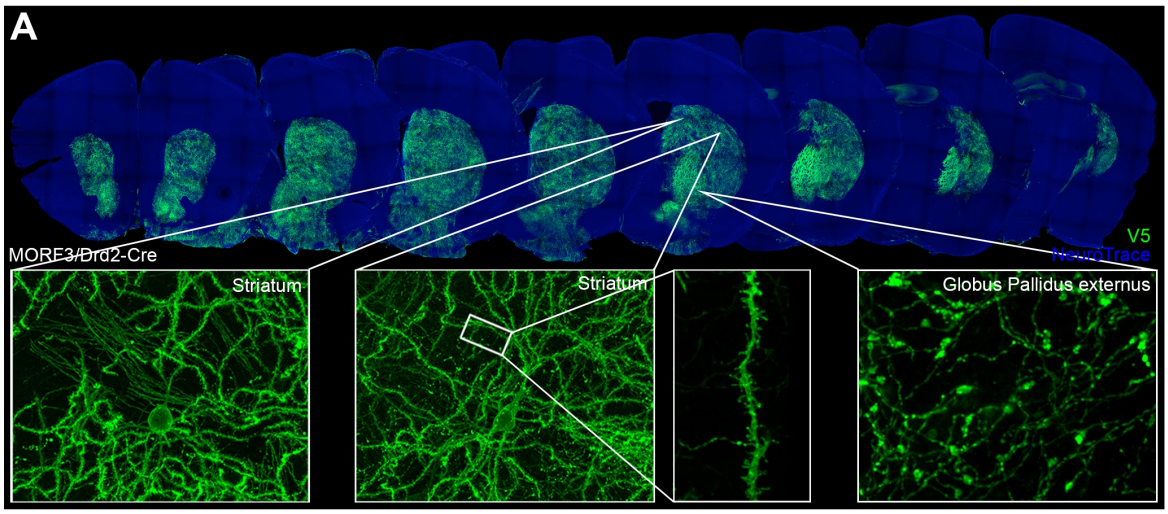

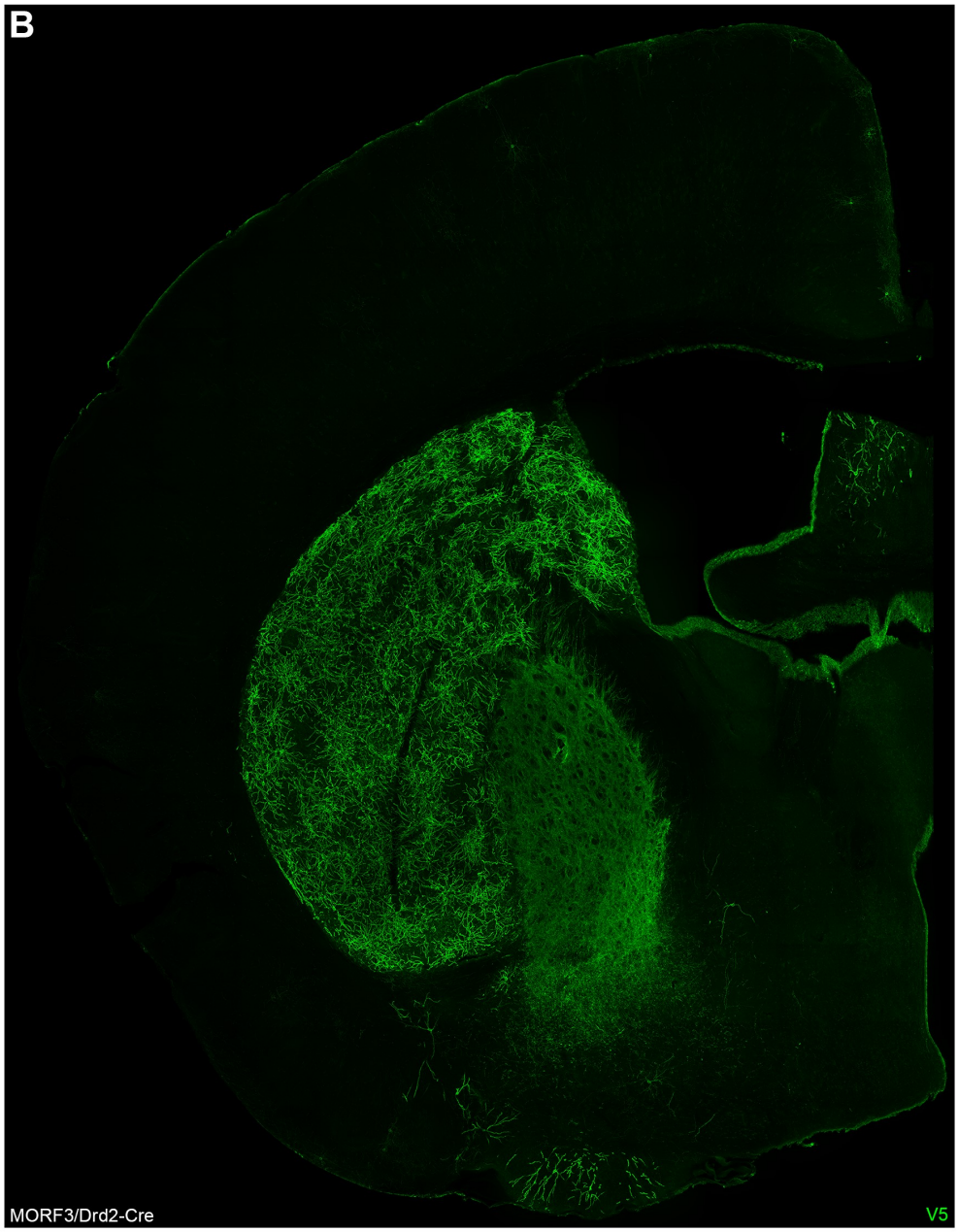

Figure S4. High-resolution images of MORF3/Drd2-Cre coronal sections. Related to Figure 3. (A) Andor DragonFly confocal imaging of 500µm-thick serial sections from MORF3/Drd2-Cre that were immunolabeled for V5 and cleared with iDISCO+ reveals detailed morphology of striatal MSNs, their dendrites in the striatum, and axons in the GPe. (B) Individual high-resolution image of a MORF3/Drd2-Cre coronal section processed with iDISCO+ and imaged at 30x with the Andor DragonFly confocal system.

Supplemental Figure 5

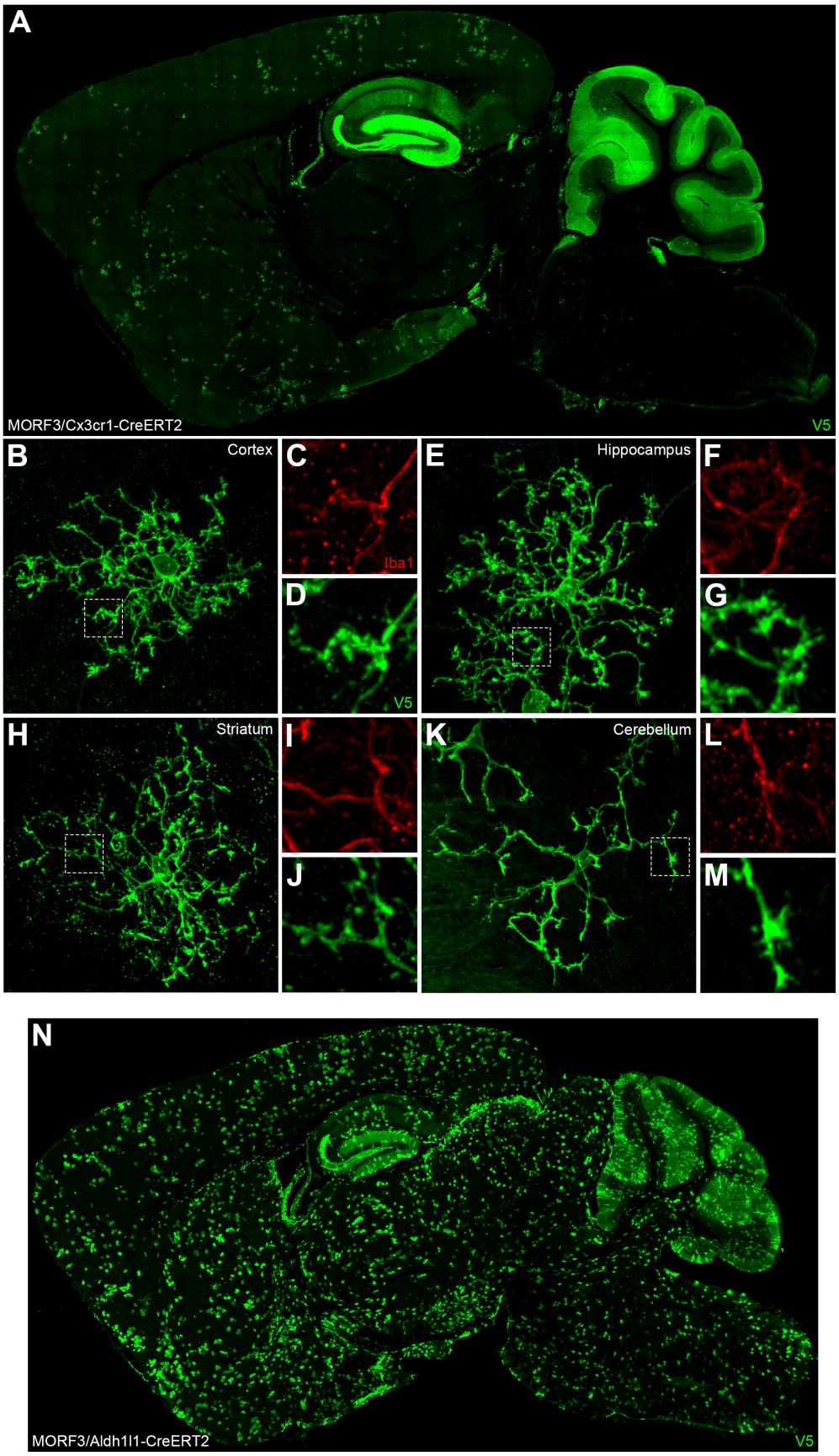

Figure S5. MORF3 labeling of microglia and astrocytes with tamoxifen-inducible CreERT2 lines. Related to Figure 4. (A) Sparse, brain-wide distribution of MORF3-labeled microglia in MORF3/Cx3cr1-CreERT2 mice induced with 100mg/kg tamoxifen for 5 days. (B-M) Representative examples of MORF3-labeled microglia from different brain regions, including the cortex (B-D), hippocampus (E-G), striatum (H-J), and cerebellum (K-M), with the magnified boxed regions showing the increased detail of the microglial processes and endfeet in MORF3-labled images compared to Iba1 immunostaining. (N) Sparse, brainwide distribution of MORF3-labeled astrocytes in MORF3/Aldh1l1-CreERT2 mice induced with 100mg/kg tamoxifen for 3 days.

Supplemental Figure 6

A

Magnification	Numerical Aperture (NA)	Field Number (mm)	Working Distance (μm)	Max section thickness (μm; excluding coverslip)
30x	1.05	22	800	650
40x	1.25	22	300	150
60x	1.3	22	300	150

B

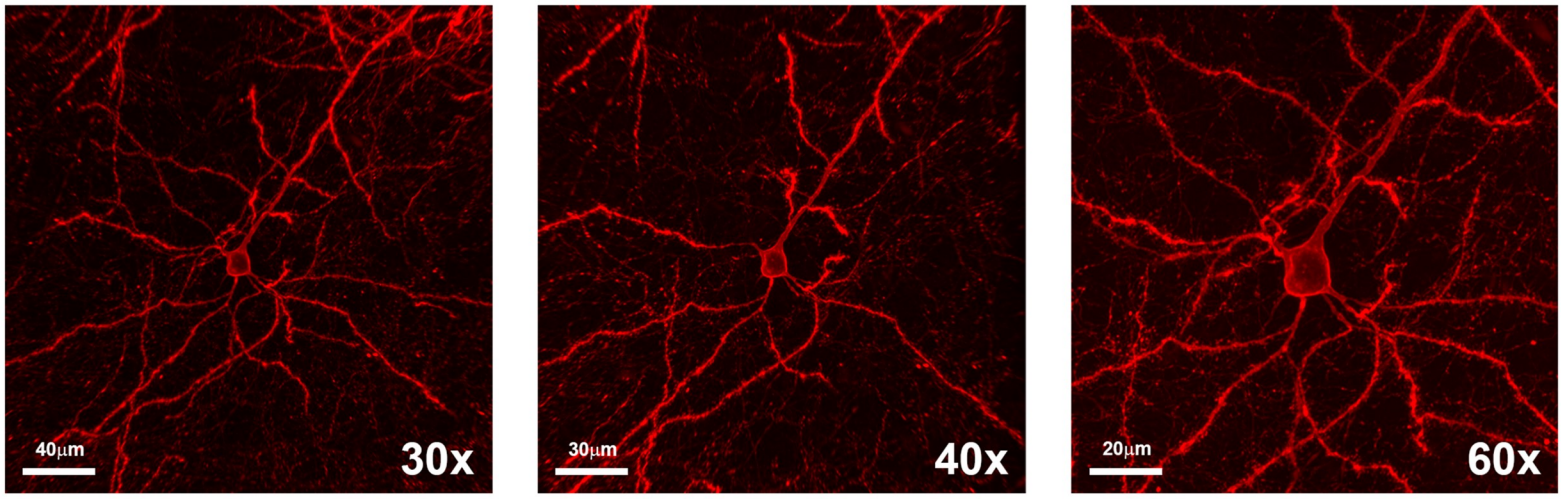

C

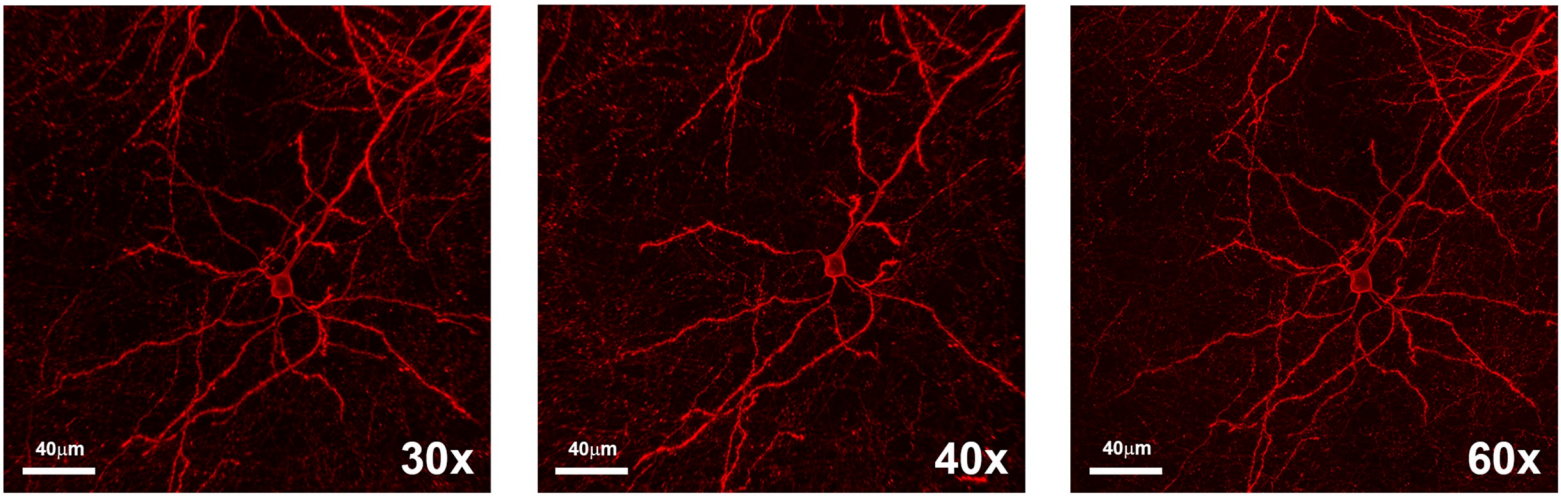

Figure S6. Comparison of Olympus silicone immersion objectives for imaging full morphology of MORF-labeled neurons in thick-sectioned, iDISCO+ cleared tissue. Related to Figure 6. (A) Table comparing the properties of three high-magnification Olympus silicone immersion objectives on the Andor DragonFly confocal system. (B) The same PN from a MORF3/CamK2a-CreERT2 imaged on the DragonFly with the 30x, 40x, and 60x objectives. At full resolution, synaptic spines can be clearly resolved on the 60x but not the 30x. (C) When the images from the 40x and 60x are scaled to the same size as the 30x, all objectives provide sufficient levels of resolution necessary to image and reconstruct fine neuronal processes. The critical difference is that the 800μm working distance of the 30x, compared to the 300μm working distance of the 40x or 60x (not accounting for the thickness of the coverslip), is required to image the full 3D morphologies of most neurons.

Supplemental Figure 7

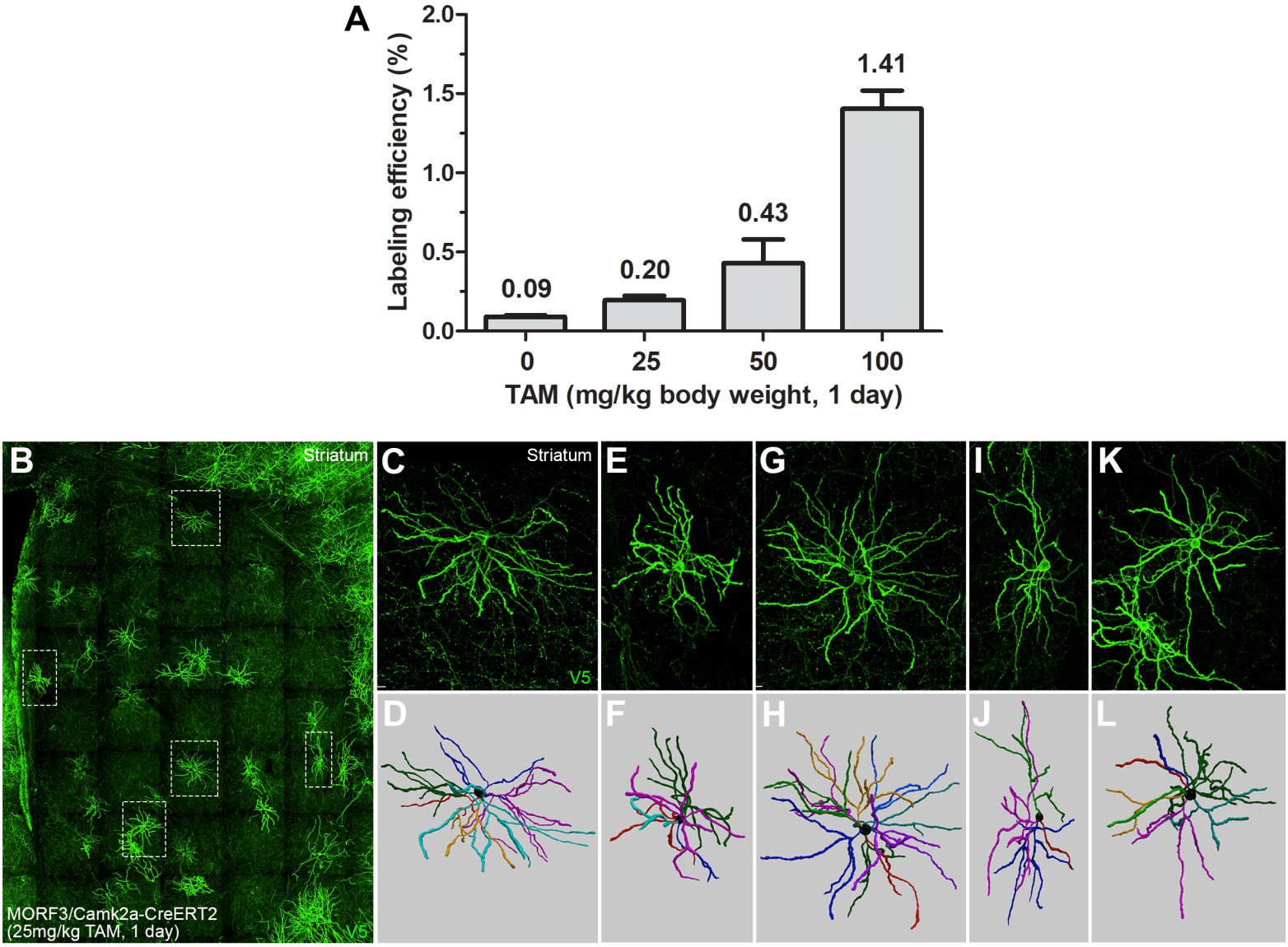

Figure S7. The labeling frequency of striatal MSNs in MORF3/Camk2a-CreERT2 can be tuned with tamoxifen to allow automated digital reconstruction and segmentation. Related to Figure 6. (A) Increasing doses of tamoxifen, from 0, to 25, 50, and 100mg/kg for 1 day in MORF3/Camk2a-CreERT2 mice increase the labeling frequency of striatal MSNs from 0.09% to 0.2%, 0.43%, and 1.41%, respectively. (B-L) Examples of very sparsely labeled MSNs and their corresponding 3D reconstructions from throughout the dorsal striatum of a MORF3/CamK2a-CreERT2 mouse induced with 25mg/kg TAM for 1 day.

Supplemental Figure 8

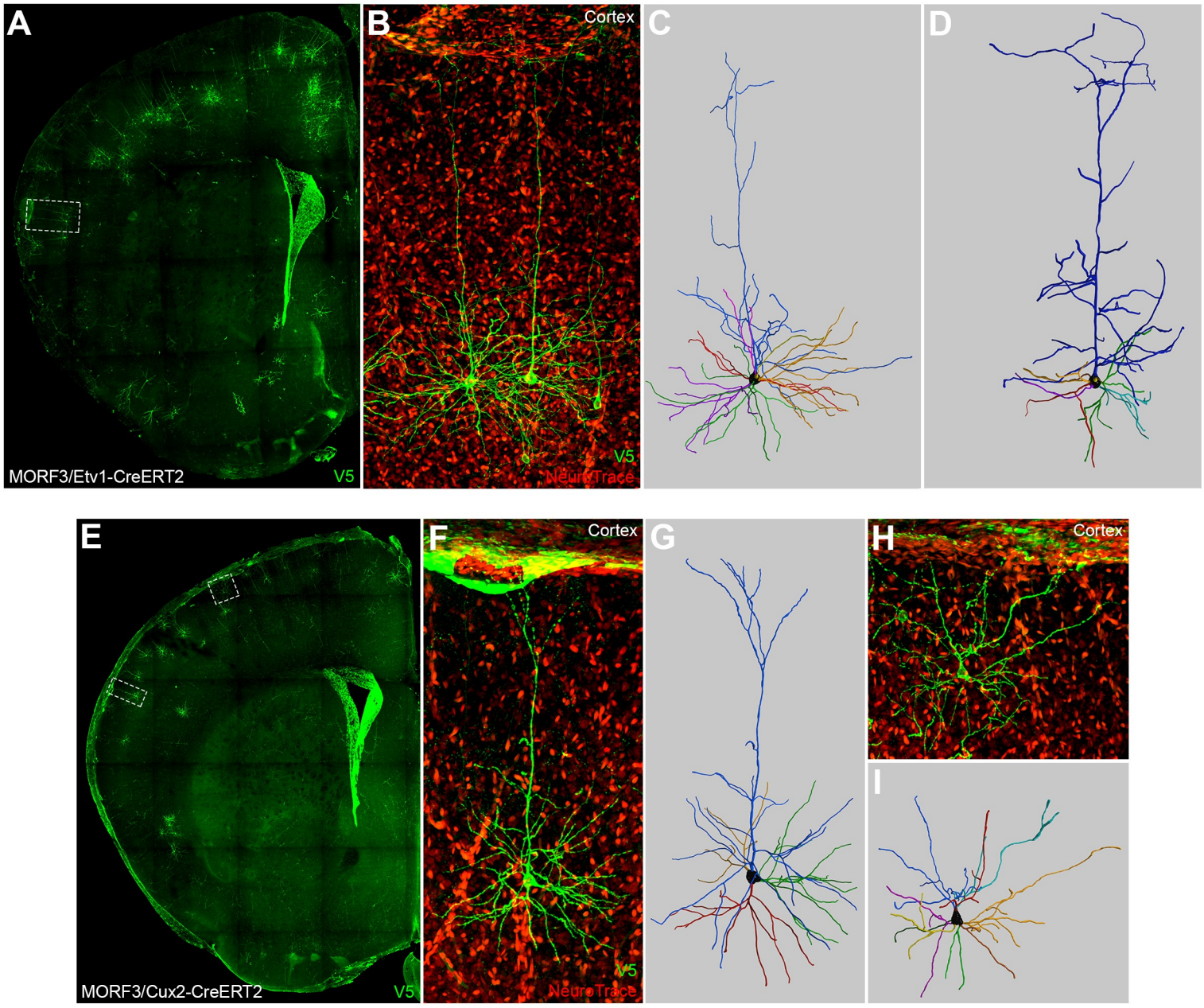

Figure S8. The labeling frequency of cortical projections neurons can be tuned down with tamoxifen to allow digital reconstruction in MORF3 mice crossed with various layer-specific cortical CreERT2-lines. Related to Figure 6. (A) Distribution of layer 5 PNs sparsely labeled in MORF3/Etv1-CreERT2 mice induced with 100mg/kg tamoxifen for 3 days. (B-D) The two intertwined layer 5 PNs (B) from the boxed region in A can be separated into individual reconstructions (C and D). (E) Sparse labeling of layer 2/3/4 PNs throughout the cortex in MORF3/Cux2-CreERT2 mice induced with 50mg/kg tamoxifen for 1 day. (F-I) Examples of MORF3-labeled layer 2/3 PNs (F and H) from the boxed regions in E and the corresponding 3D reconstructions (G and I).

Supplemental Figure 9

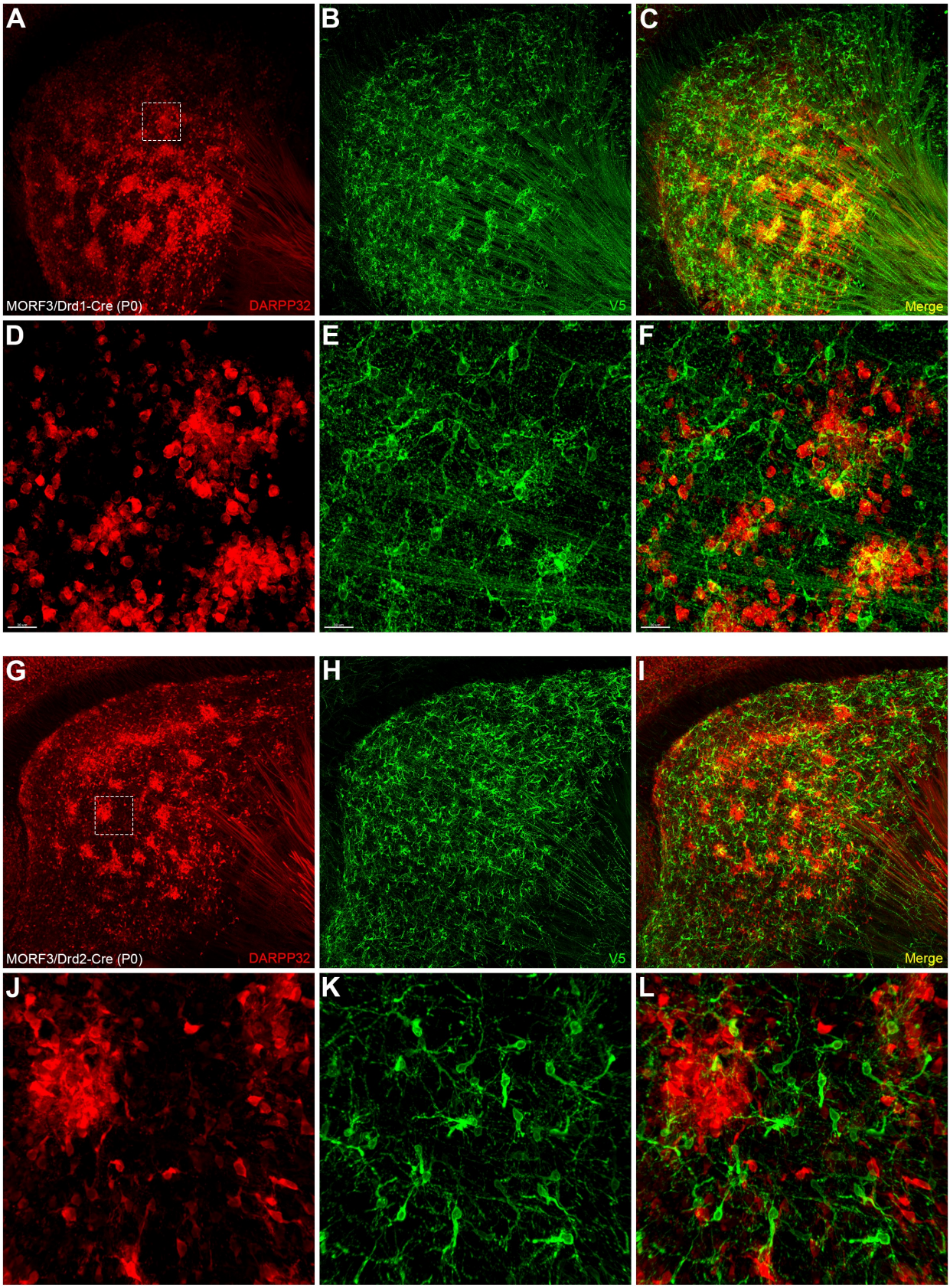

Figure S9. Sparse immunolabeling of striatal D1- and D2-MSNs at P0 in MORF3/Drd1-Cre and MORF3/Drd2-Cre mice, respectively. Related to Figure 7. (A-C) Distribution of MORF3-labeled D1-MSNs, co-labeled with DARPP32, in the developing striatum of a MORF3/Drd1-Cre mouse at P0. (D-F) Higher magnification of the boxed region in A reveals morphological details of P0 D1-MSNs in the developing patch and matrix, as demarcated by the concentrated clusters of DARPP32 expression. (G-I) Distribution of MORF3-labeled D2-MSNs, co-labeled with DARPP32, in the developing striatum of a MORF3/Drd2-Cre mouse at P0. (J-L) Higher magnification of the boxed region in G reveals morphological details of P0 D2-MSNs in the developing patch and matrix, as demarcated by the concentrated clusters of DARPP32 expression.

Supplemental Figure 10

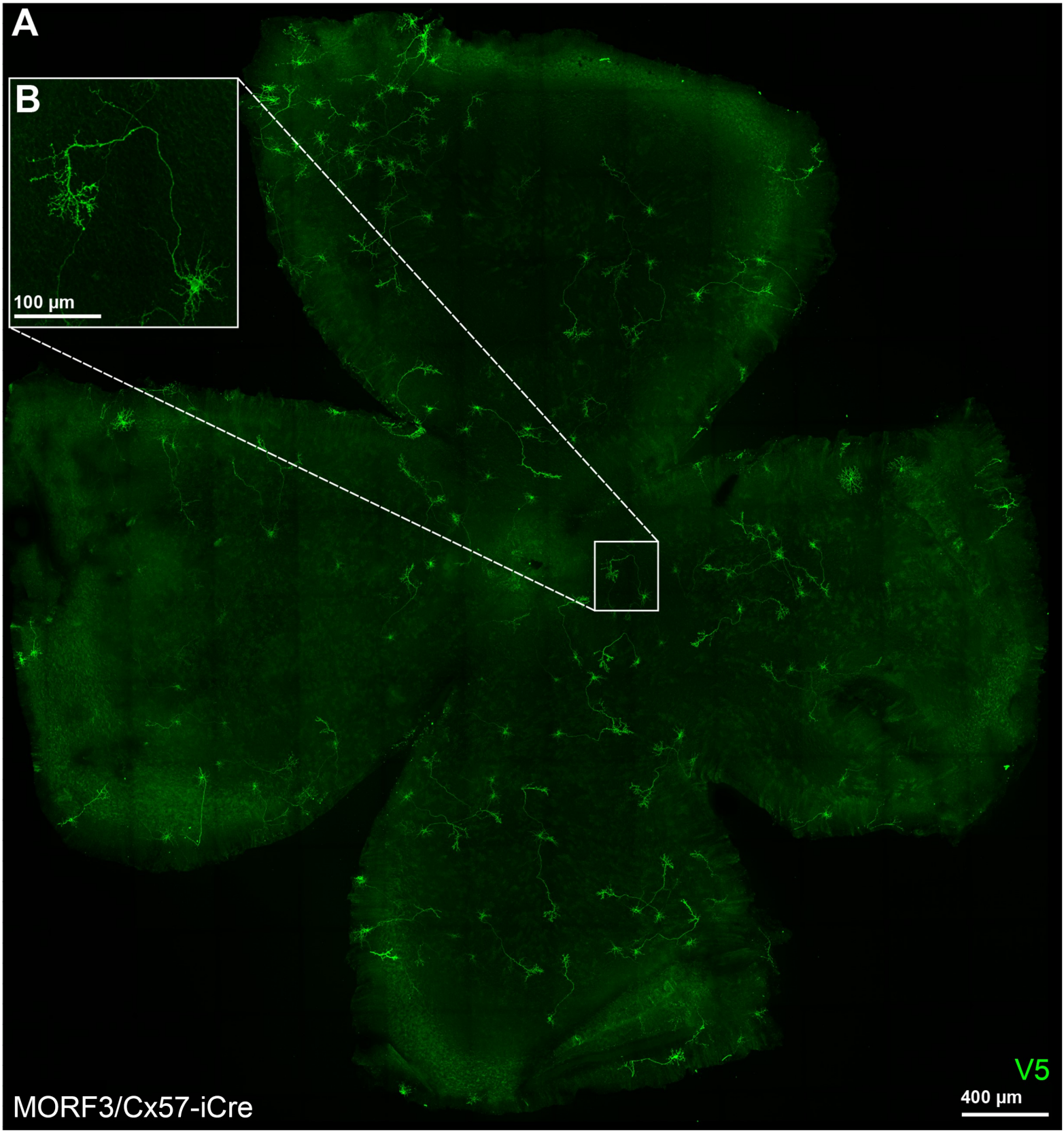

Figure S10. Retina whole mount of MORF3/Cx57-iCre at P5 demonstrating sparse, complete, and mostly non-overlapping labeling of retinal horizontal cells. Related to Figure 7. (A) Whole flat mounted retina from a MORF3/Cx57-iCre mouse at P5, stained with anti-V5 antibody to label horizontal cells with green fluorescence. (B) Higher magnification image of the complete morphology of a single HC in the boxed region in A. Scale bars = 400µm (A), 100µm (B).

Supplemental Figure 11

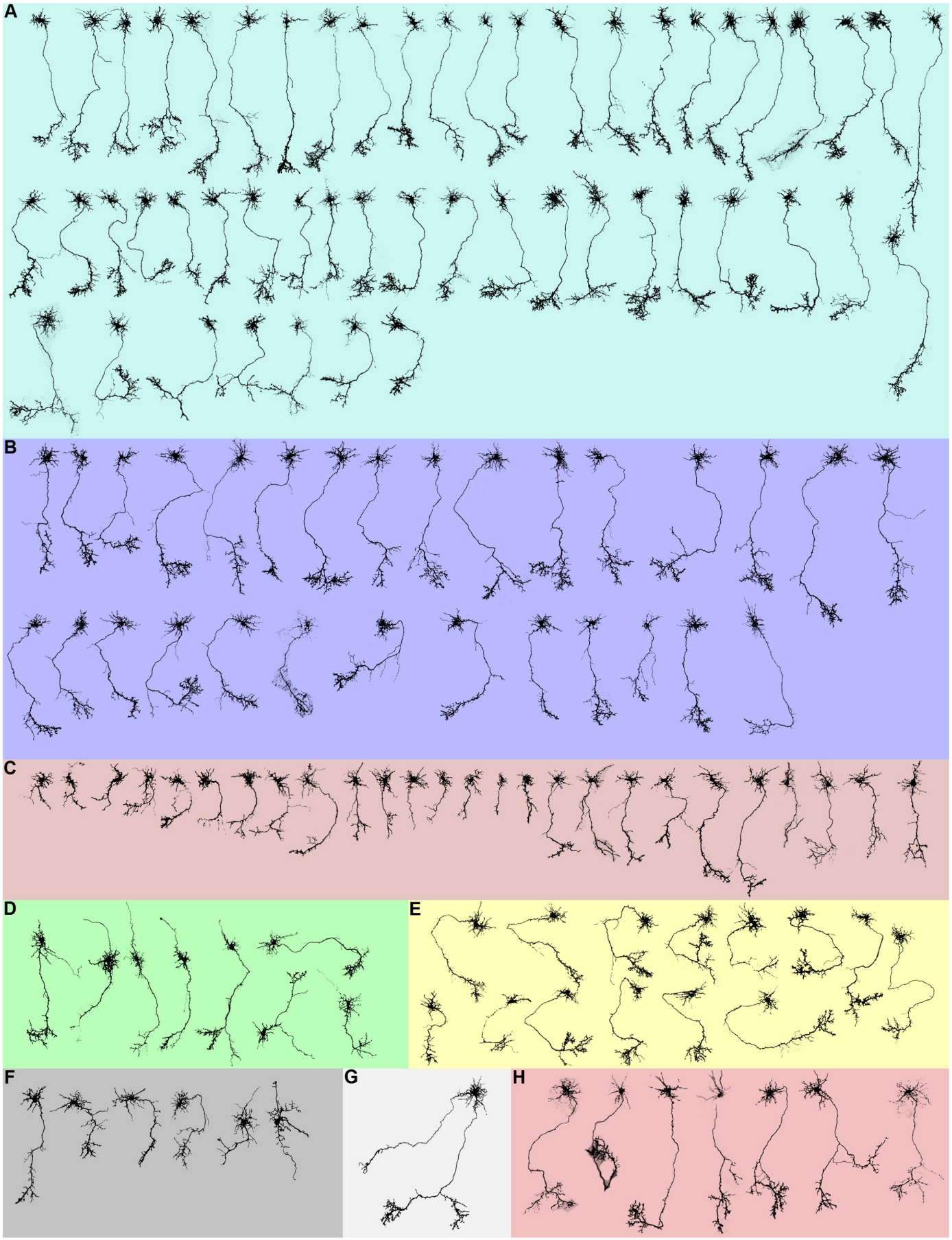

Figure S11. Summary of single cell morphology of MORF3/Cx57-iCre retinal horizontal cells at P5. Related to Figure 7. (A-H) Retinal horizontal cells reconstructed and quantitatively analyzed. Images were produced by binarizing a maximum intensity projection of the retinal horizontal cell. Background colors are according to module colors described in the main text: (A) is turquoise, (B) is blue, (C) is brown, (D) is green, (E) is yellow, (F) is black, (G) is grey, and (H) is red. (n = 142).

Supplemental Figure 12

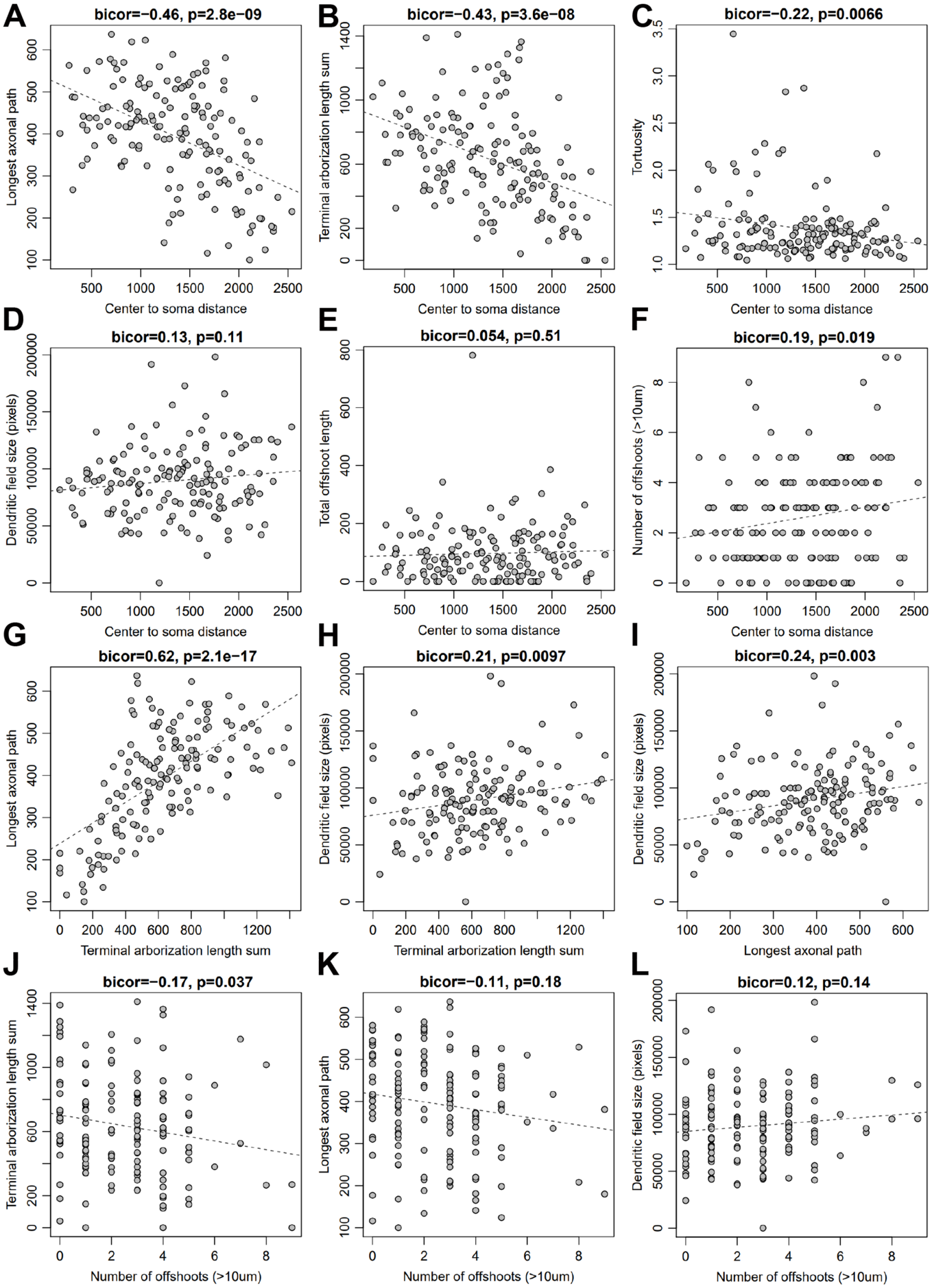

Figure S12. Concordance plots of morphological features extracted from reconstructed MORF3/Cx57-iCre retinal horizontal cells. Related to Figure 7. Concordance plots of morphological features extracted from 3D retinal horizontal cell reconstructions (n = 152 cells).

Supplemental Table 1

Table S1. TIGRE-MORF breeding results in non-Mendelian offspring ratio in some Cre-driver line heterozygous crosses.

Cre line	Cell type	MORF$^+$	Cre$^+$	MORF$^+$/ Cre$^+$	Wild type	p-value
Drd1-Cre	Direct Striatal MSN	6 (5)	10 (5)	0 (5)	4 (5)	0.015 *
Adora2a-Cre	Direct and Indirect Striatal MSN	9 (6.75)	6 (6.75)	0 (6.75)	12 (6.75)	0.009 **
Rbp4-Cre	Cortical layer V neurons	12 (6.25)	3 (6.26)	0 (6.25)	10 (6.25)	0.001 **
Camk2a-CreERT2	Excitatory cortical neurons	19 (14)	14 (14)	7 (14)	16 (14)	0.134
TH-Cre	Dopaminergic neurons	3 (4.75)	7 (4.75)	5 (4.75)	4 (4.75)	0.606

Expected genotype abundance in parenthesis (χ^2 Test); * $p < 0.05$, ** $p < 0.01$

Table S1. Breeding results from TIGRE-MORF line crossed with different Cre lines compared to expected Mendelian ratios. Related to Table 1.

Supplemental Table 2

Table S1. Summary of MORF Mouse Lines Crossed with Different Cre Lines		
Cre line	**MORF line**	**Mice imaged**
Drd1-Cre	MORF1	2
Drd2-Cre	MORF1	2
Rgs9-Cre	MORF1	3
TH-Cre	MORF1	2
EIIa-Cre	MORF1	2
Pcp2-Cre	MORF1	1
Pvalb-Cre	MORF1	1
Nestin-Cre	MORF1	1
TH-Cre	TIGRE-MORF	4
Camk2-CreERT2	TIGRE-MORF	2
A2a-Cre	MORF2	1
Drd1-Cre	MORF2	4
Drd2-Cre	MORF2	6
Pcp2-Cre	MORF2	3
Pvalb-Cre	MORF2	3
Rgs9-Cre	MORF2	4
Cx57-iCre	MORF2	2
Cx57-iCre (P5)	MORF2	2
Cx57-iCre (P10)	MORF2	3
Cx57-iCre (P15)	MORF2	3
Kcng4-Cre	MORF2	4
Rbp4-Cre	MORF3	8
Drd1-Cre	MORF3	10
Drd1-Cre (P0)	MORF3	2
Drd2-Cre	MORF3	22
Drd2-Cre (P0)	MORF3	2
Cx57-iCre	MORF3	3
Cx57-iCre (P5)	MORF3	7
Cx57-iCre (P4)	MORF3	4
Cx57-iCre (P10)	MORF3	2
Pcp2-Cre	MORF3	2
Pvalb-Cre	MORF3	6
Pvalb-Cre (P0)	MORF3	2
Pvalb-Cre (P17)	MORF3	2
SST-Cre	MORF3	2
Cx3cr1-CreERT2	MORF3	7
Aldh1l1-CreERT2	MORF3	2
Etv1-CreERT2	MORF3	7
Cux2-CreERT2	MORF3	5
Camk2-CreERT2	MORF3	28
VIP-Cre	MORF3	4
Nestin-Cre	MORF3	2
	Total	**184**

Table S2. Total number of mice generated from MORF lines crossed with different Cre lines to examine sparse Cre-dependent MORF-labeling. Related to Table 1.